Properties and corrosion behaviour of reactive magnetron sputtered TiAlN coatings on AISI 316L SS in simulated bodily fluid

B. Subramanian*[1], G. Umamaheswari[2] and M. Jayachandran[1]

Because of their superior properties, titanium aluminium nitride (TiAlN) films are increasingly applied as protective layers on cutting and forming tools and turbine compressor blades and as biocompatible barriers. TiAlN films were deposited on AISI 316L stainless steel substrates by reactive magnetron sputtering using a target consisting of equal segments of titanium and aluminium. X-ray diffraction characterisation showed that the coating structure was face centred cubic. AFM and SEM studies indicated that the coatings are regular with dense shpherical granular structure. The coatings were also characterised using photoluminescence spectroscopy and Raman microscopy to elucidate the optical and acoustic phonon modes of the cubic lattices. Characteristic peaks were observed at 250, 620 and 1180 cm^{-1} in laser Raman studies. Polarisation and impedance spectroscopy studies on TiAlN and TiN coated specimens were conducted in Fusuyama simulated body fluid. The charge transfer resistance R_{ct} increased in the order: uncoated 316L substrate; 2 μm TiN film; 3 μm TiN film; 2 μm TiAlN film. Thus, the TiAlN coating has the highest corrosion resistance, and was also found to have the most noble corrosion potential and lowest corrosion rate in the polarisation tests.

Keywords: Titanium aluminium nitride films, Magnetron sputtering, PVD, Corrosion resistance, Simulated bodily fluid, Biocompatible coatings

Introduction

Titanium aluminium nitride (TiAlN) coatings have been widely developed for many application fields such as cutting, forming tools, semiconductor devices, optical instruments, compressor blades of aero engines, diffusion and biocompatible barriers.[1–5] TiAlN layers have been shown to exhibit good mechanical and technical characteristics, such as good oxidation resistance at high temperature (800°C compared with 600°C for TiN layers),[6] low thermal conductivity, high microhardness (35 GPa compared with 22 GPa for TiN),[6] high wear and corrosion resistance and lower coefficient of friction.[7–9] Furthermore, TiN/Ti_2N layers have been reported to offer new possibilities to produce non-toxic human fibroblast compatible surface layers on titanium alloys.[10]

Many studies have reported on the deposition and properties of TiAlN coating produced by various fabrication techniques by physical vapour deposition (PVD) and chemical vapour deposition (CVD) such as cathodic arc plasma deposition,[11] Plasma assisted chemical vapour deposition,[12] electron beam evaporation evaporation,[13] arc ion plating,[14] reactive dc magnetron sputtering[15] and combined cathodic steered arc etching/unbalanced magnetron sputtering.[16] Higher cutting speed can be obtained with TiAlN coating, by decreasing the thermal loading of the substrate.[17] The improved hardness and better cutting performance especially in higher cutting speed range of the film, deposited by reactive dc magnetron sputtering, have been attributed to shrinkage in the lattice parameters caused by the replacement of larger titanium atoms by smaller aluminium atoms.[15]

TiAlN/CrN, a superlattice coating has proved the onset of severe oxidation can be raised to temperature as high as 900°C.[18] Hardness enhancement is found in TiAlN/VN nanomultilayers, deposited by multitarget magnetron sputtering and their hardness depend strongly on the modulation period and corresponding microstructures. The inhibition of dislocation motion by alternating strain fields is probably responsible for the improvement of hardness in the multilayer.[19]

The corrosion rate of TiAlN coating fabricated by hollow cathode ionic plating (HCIP) showed an excellent corrosion resistance in acid and salt solution, during the long term immersion test. This coating seemed to posses certain self-repairing function, because the corrosion process was obstructed by the corrosion product of Al on the interface between the coating and substrate.[20] In this investigation, the materials properties and electrochemical corrosion behaviour of dc magnetron sputtered TiAlN films on AISI 316L SS substrates are reported.

[1]ECMS Division, Central Electrochemical Research Institute, Karaikudi 630 006, India
[2]Center for Education, Central Electrochemical Research Institute, Karaikudi 630 006, India

*Corresponding author, email tspsenthil@yahoo.com

Published by Maney on behalf of the Institute
Received 5 April 2007; accepted 15 June 2007
DOI 10.1179/174327807X234723

Experimental

The layers of TiAlN were deposited on well cleaned AISI 316L stainless steel substrates using a dc magnetron sputter deposition unit HIND HIVAC. The base vacuum of the chamber was below 1×10^{-6} torr at the substrate temperature of 400°C. A high purity argon was fed into the vacuum chamber for the plasma generation. The substrates were etched for 5 min at a dc power of 50 W and an argon pressure of 10 mtorr (1·33 Pa). The deposition parameters for TiAlN sputtering are summarised in Table 1.

The deposited films were analysed for crystallographic structure with a diffractometer using Cu K_α radiation. The surface of the coating was characterised by scanning electron microscopy (SEM) using a Hitachi S 3000H microscope equipped with an energy dispersive X-ray (EDX) spectrometer and a molecular imaging atomic force microscope (AFM). Microhardness of the films on steel was evaluated by using a DM-400 microhardness tester from LECO with Vickers indenter. A dwell time of 15 s and loads of 25 g and 5 g were used for the measurement. The excitation wavelength was 632·8 nm for Raman measurements. The data were collected with a 10 s data point acquisition time in the spectral region of 200–1200 cm^{-1}.The photoluminescence (PL) measurements were made using a Cary eclipse fluorescence spectrophotometer (VARIAN) employing a PbS photodetector and a 150 W xenon arc discharge lamp as the excitation light source.

Electrochemical corrosion testing

Electrochemical polarisation studies were carried out using BAS IM6 electrochemical analyser. Experiments were conducted using the standard three electrode configuration, with a platinum foil as a counter electrode, saturated calomel electrode as reference electrode and the sample as a working electrode. Specimens (1·0 cm^2 exposed area) were immersed in the test solution of modified Fusayama simulated bodily fluid.[21] Experiments were carried out at room temperature (28°C). In order to establish the open circuit potential (OCP), before measurements, the sample was immersed in the solution for ~60 min.

Impedance measurements were conducted using a frequency response analyser. The spectrum was recorded in the frequency range of 10 mHz–100 kHz. The applied alternating potential had a root mean square amplitude of 10 mV on the open circuit potential. After obtaining a stable OCP the upper and lower potential limits of linear sweep voltametry were set at ±200 mV with respect to OCP. The sweep rate was 1 mV s^{-1}. The Tafel plots were obtained after the electrochemical measurements.

Table 1 Deposition parameters for TiAlN dc reactive magnetron sputtering

Objects	Specification
Target	Ti (99·9%) and Al (99·9%)
Substrate	AISI 316L SS, glass
Target to substrate distance	50 mm
Ultimate vacuum	1×10^{-6} mbar
Operating vacuum	2×10^{-3} mbar
Sputtering gas ($Ar : N_2$)	50 : 50
Power	300 W
Substrate temperature	400°C

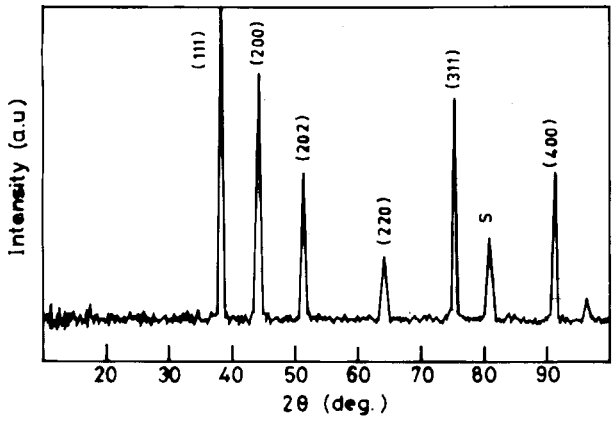

1 X-ray diffractogram of sputtered TiAlN film on steel

The porosity was determined from the polarisation resistance and corrosion potential deduced from the potentiodynamic polarisation technique using the relation[22]

$$P = (R_{ps}/R_p) \times 10 - |\Delta E_{corr}|/b_a \quad (1)$$

where P is the total coating porosity, R_{ps} is the polarisation resistance of the substrate, R_p is the polarisation resistance of the coated steel, ΔE_{corr} is the difference between the corrosion potentials of the coated AISI 316L SS and the bare AISI 316L SS substrate, and b_a is the anodic Tafel slope of the substrate.

Results and discussion

Structural and microstructural analyses

The XRD pattern obtained for the reactive magnetron sputter deposited titanium aluminium nitride films on AISI 316L SS with the Ar/N_2 ratio of 50 : 50 (Fig. 1) indicated a successful formation of TiAlN which have a face centred cubic crystal system with the lattice parameter of a=4·231 nm and belong to a space group of Fm3m. The data show that the observed 'd' values are in very good agreement with the values reported by other investigators.[23] The peaks at 36·780 and 42·539 corresponding to diffraction along (111) and (200) plane.

The grain size of the film was found to be ~30 nm. Such a small grain size contributes to the smooth surface morphology and also may have a beneficial effect on the improvement of the microhardness of the coating.[24] Also the grain size reduction to the nanometre range results in considerable improvement in their resistance to localised corrosion.[25] The value of microstrain (ε) and the dislocation density (δ) of the as grown film were found to be $5{\cdot}065 \times 10^{-4}$ and $2{\cdot}0269 \times 10^{14}$ lin m^{-2}. Internal residual stresses could be built up in the deposited films due to lattice mismatch between the film structure and the substrate surface.

The surface topography of these TiAlN thin films was studied using AFM for a scanned area of 10×10 μm and the section analysis method that allows the determination of the profile of the samples with a line drawn over the surface as shown in Fig. 2. From the horizontal cross-section analysis, the minimum and maximum globule size was estimated to be in the range of 30–60 nm and some shallow valleys of ~30 nm depth were observed.

Roughness analysis of the coating was carried out and the value of the mean roughness R_a was calculated as the

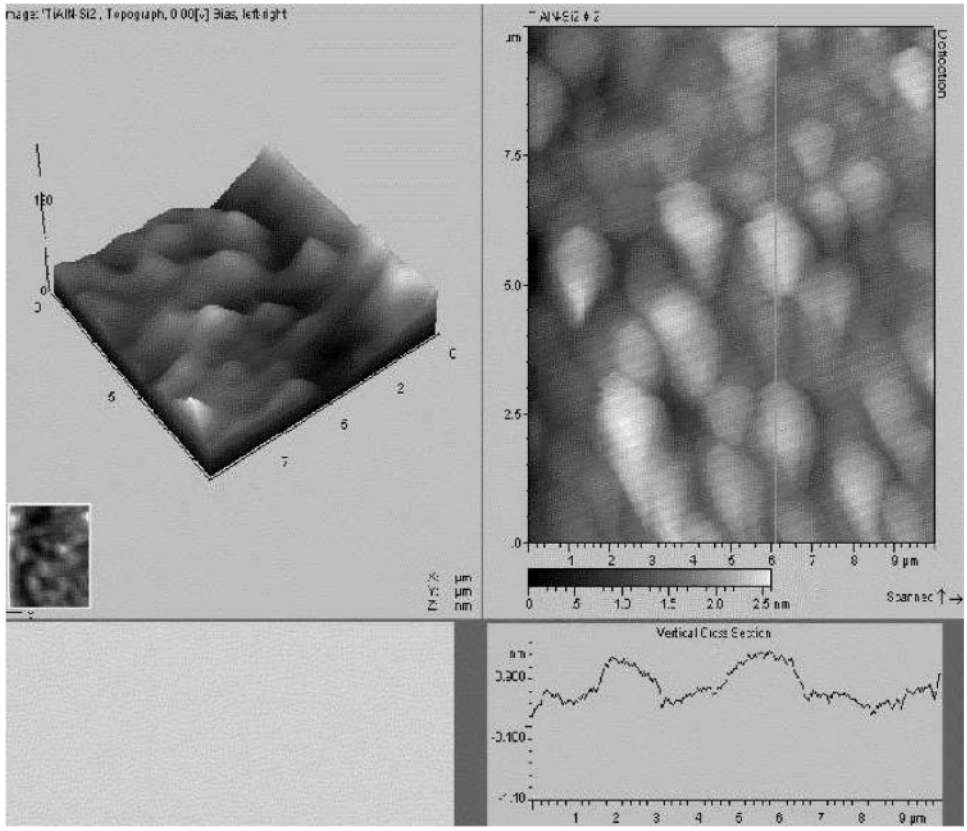

2 Image (AFM) showing topography of TiAlN film on steel

deviations in height from the profile mean value.[26] The value, estimated from these images was ~12 nm which shows that the films were smooth in nature.

Scanning electron microscopy topography of the TiAlN coated AISI 316L SS substrate is shown in Fig. 3. Only a very few pits were observed over the surface, indicating the surface was homogeneous, uniform and dense. The deposit compositions analysed using energy dispersive spectroscopy (EDS) were found to be 36·22% for Ti, 29·30% for Al, 33·08% for N, 0·71% for Ar and 0·69% for O. In addition to constituent elements traces of argon and oxygen were also detected in the EDS data. *In situ* Ar^+ ion bombardment of the growing film could be reason for the incorporation of Ar and oxygen could be because of very thin oxide layer formed on the surface of the film. It may also be due to an incipient corrosion process during handling the sample.

The surface microhardness values of TiAlN films on AISI 316L SS were measured using a Vickers diamond indenter at a load of 25 and 10 g for 15 s. The mean values, 2800 HV0·01 and 2720 HV0·025, were calculated. Nearly the same values were found for all the samples.

Photoluminescence and laser Raman studies

A room temperature PL spectrum of the titanium aluminium nitride film is shown in Fig. 4. It is

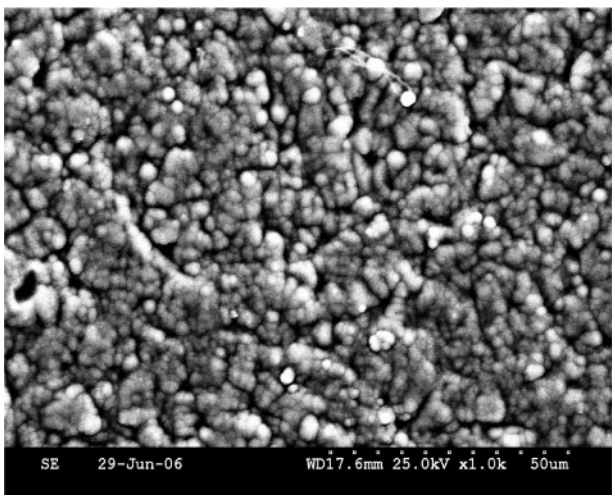

3 Plane view of sputtered TiAlN film on steel

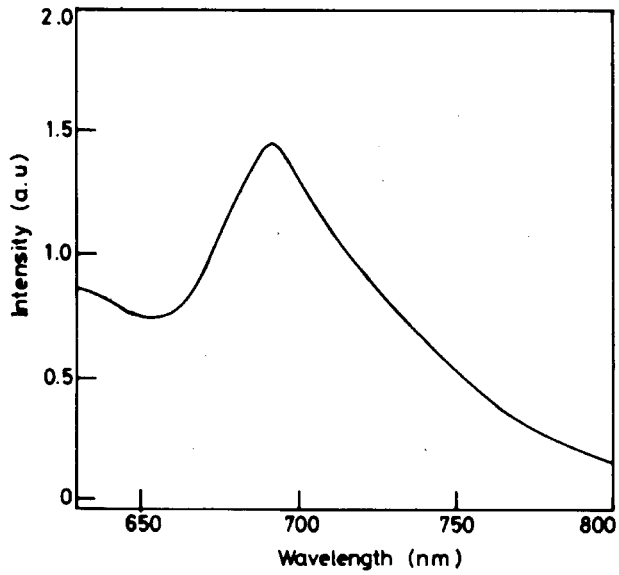

4 Photoluminescence spectrum obtained for magnetron sputtered titanium aluminium nitride film

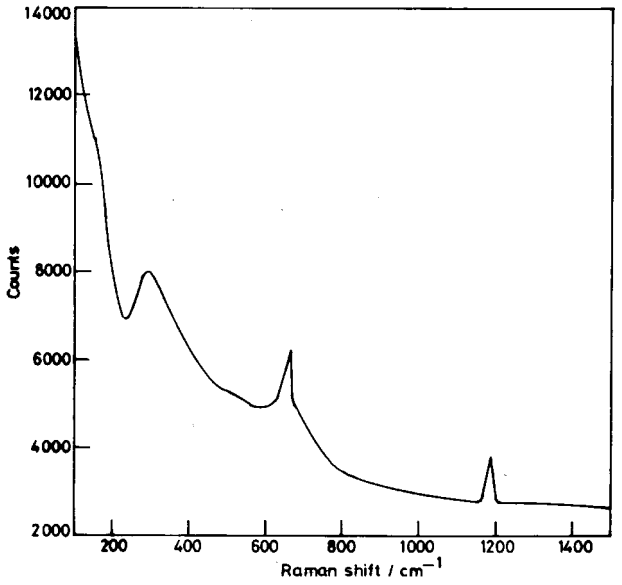

5 Laser Raman spectrum obtained for titanium aluminium nitride film

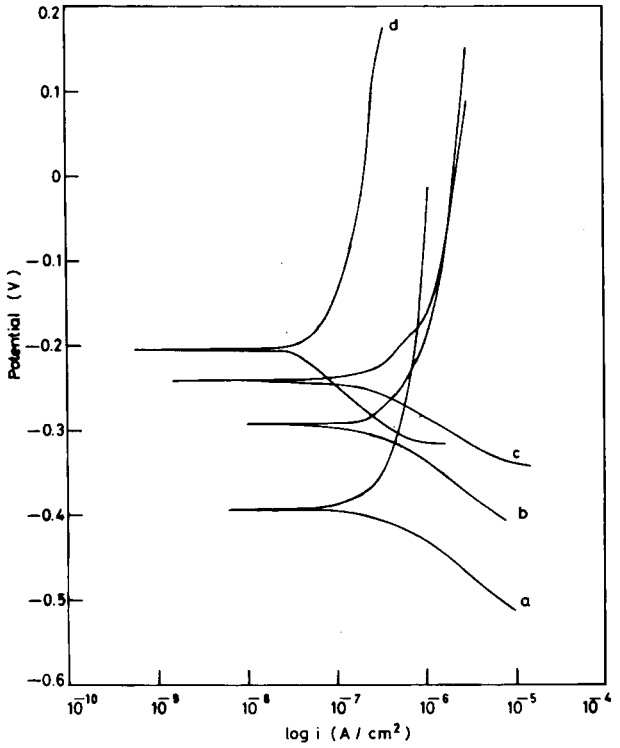

6 Polarisation studies of *a* blank substrate, *b* TiN (2 μm), *c* TiN (3 μm) and *d* TiAlN (2 μm) in simulated bodily fluid

interesting to note that emission appearing at 690 nm is only in the visible region. This implies that the TiAlN films prepared by dc reactive magnetron sputtering are of good optical quality. The scattering in the acoustic range was primarily determined by the vibrations of the heavy Ti ions (typically 150–300 cm^{-1}) and in the optic range by vibrations of the lighter N ions (typically 400–650 cm^{-1}). As the lattice gets more complex, e.g. on going from TiN to TiAlN, it is observed that the total spectral density in the gap region (380–500 cm^{-1}) between the acoustic and optic modes increases.

The characteristic peaks at 250, 620 and 1180 cm^{-1}, related to transverse acoustic (TA)/longitudinal acoustic (LA), transverse optical (TO)/longitudinal optical (LO) and second order optical (2O) modes of TiAlN respectively, were observed in the Raman spectra of TiAlN films (Fig. 5) prepared by reactive sputtering process. This is in good agreement with the reported values for TiAlN films by Constable *et al.*[27]

Potentiodynamic polarisation and ac impedance spectroscopy

Typical polarisation curves obtained for the corrosion behaviour of the samples are shown in Fig. 6. Table 2 shows the results of corrosion testing for the AISI 316L stainless steel substrate and specimens coated with TiN (2 μm), TiN (3 μm) and TiAlN (2 μm) in simulated bodily fluid solution. The corrosion potential of the AISI 316L SS substrate is about −0·393 V. The corrosion current I_{corr} of steel substrate is greater than those of TiN (2 μm), TiN (3 μm) and TiAlN (2 μm). For the TiAlN, the corrosion current is reduced to 0·21 μA cm^{-2}, as indicated in Table 2. The porosity and the corrosion rate of the TiAlN coating on AISI 316 L SS substrate were found to be much lower than those of the TiN coatings on substrate and bare substrate.

The same three electrode cell assembly, as used for the potentio dynamic polarisation experiments, was employed for the ac impedance investigations. Impedance measurements were made at OCP applying an ac signal of 10 mV in the frequency range 10 Hz to 1 MHz. The Nyquist plots (Fig. 7) showed a single semicircle for all the samples. At higher frequencies, the interception of real axis in the Nyquist plot is ascribed to the solution resistance (R_s) and at the lower frequencies, the interception with the real axis is ascribed to the charge transfer resistance (R_{ct}). The double layer capacitance C_{dl} value is obtained from the frequency at which Z imaginary is maximum

$$\omega(Z_{(im)}\max) = 1/C_{dl}R_{ct} \quad (2)$$

When the sample is immersed in the electrolyte, the defects in the coating provide the direct diffusion path for the corrosive media. In this process, the galvanic corrosion cells are formed and the localised corrosion dominates the corrosion process. The proposed equivalent circuit for such a system is shown in the Fig. 8. The parameters in the equivalent circuit R_{pore} and C_{coat} are related to the properties of the coating and the electrolyte/coating interface reactions. R_{ct} and C_{dl} are

Table 2 Potentiodynamic polarisation data of AISI 316LSS (substrate), TiN (2 μm)/substrate TiN (3 μm)/substrate and TiAlN (2 μm)/substrate

Sample	E_{corr}, V	b_a, V dec^{-1}	b_c, V dec^{-1}	I_{corr}, A cm^{-2}	Porosity, %	Corrosion rate, mpy
AISI 316LSS (substrate)	−0·393	2·45	−0·21	$4{\cdot}2\times10^{-6}$	–	1·97
TiN (2 μm)/substrate	−0·294	0·63	−0·11	$7{\cdot}7\times10^{-7}$	0·4122	1·18
TiN (3 μm)/substrate	−0·243	0·68	−0·11	$9{\cdot}1\times10^{-7}$	0·2406	1·38
TiAlN (2 μm)/substrate	−0·215	0·78	−0·13	$1{\cdot}2\times10^{-7}$	0·0225	0·26

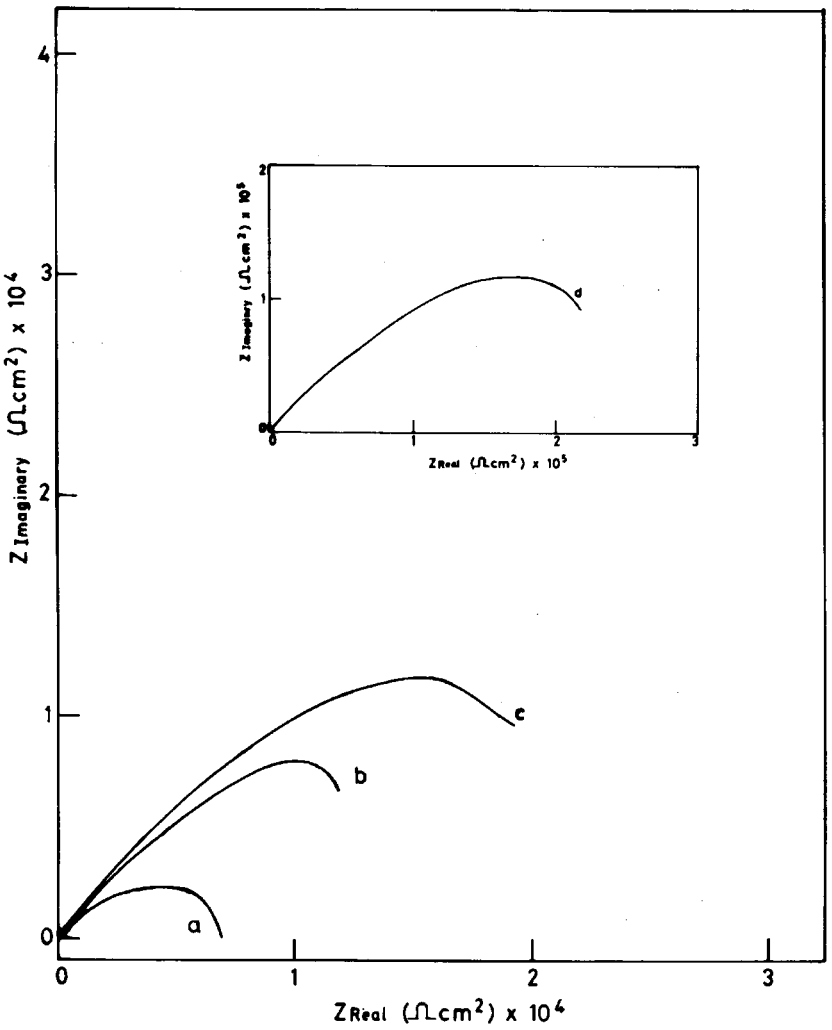

7 Nyquist plots for corrosion measurements of *a* blank substrate, *b* TiN (2 μm), *c* TiN (3 μm) and *d* TiAlN (2 μm) in simulated bodily fluid

related to the charge transfer reaction at the electrolyte/substrate interface. When the sample is immersed in the electrolyte the defects in the coating provide the direct diffusion path for the corrosive media. The electrochemical interface can be divided into two subinterfaces: electrolyte/coating and electrolyte/substrate.

The single semicircle behaviour obtained for the samples is believed to be due to the short exposure time (60 min), which is not sufficient to reveal the degradation of the substrate.[28]

The R_{ct} increases (Table 3) in the following order: steel substrate<TiN (2 μm)/substrate<TiN (3 μm)/substrate<TiAlN (2 μm)/substrate, which shows that TiAlN coating on steel substrate has higher corrosion resistance. Figure 9 (log |Z| versus log *f* plot) indicates that the absolute impedance measurements are in the same order.

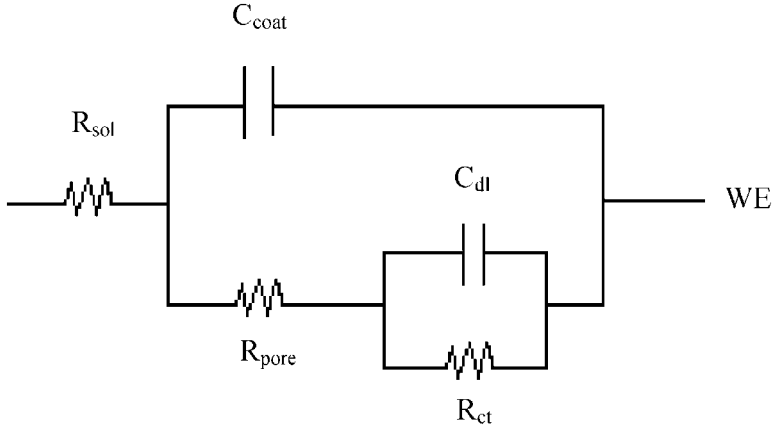

8 Equivalent circuit used for fitting electrochemical impedance data

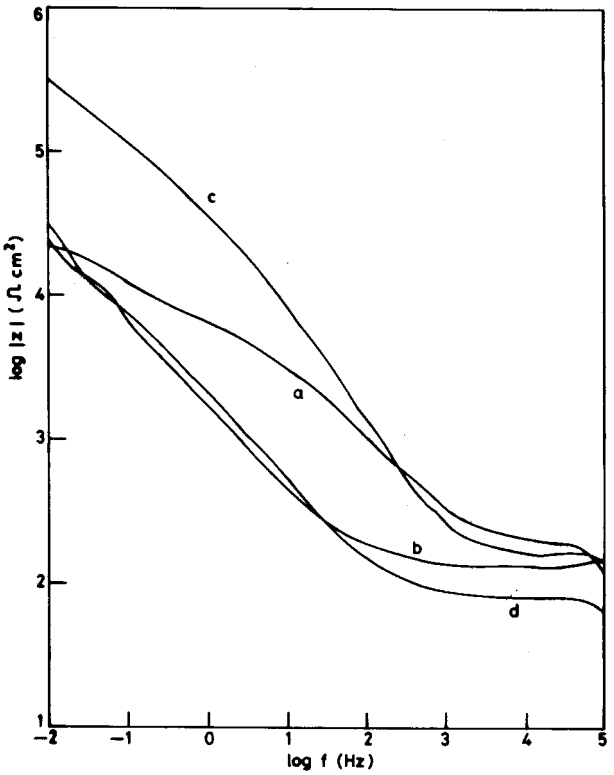

9 Bode plots (log |Z| versus log *f*) of *a* blank substrate, *b* TiN (2 μm), *c* TiN (3 μm) and *d* TiAlN (3 μm) in simulated bodily fluid

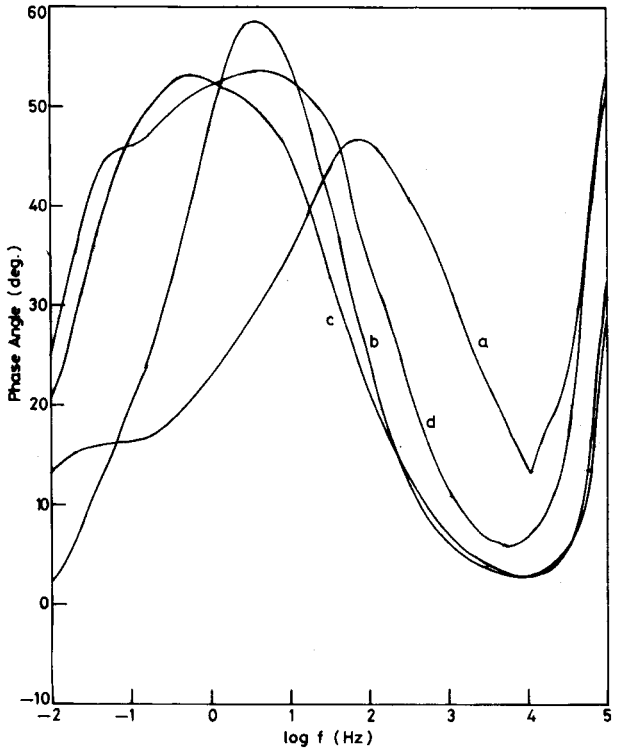

10 Bode plots (log *f* versus phase angle) of *a* blank substrate, *b* TiN (2 μm), *c* TiN (3 μm) and *d* TiAlN (3 μm) in simulated bodily fluid

The Bode plot (log *f* versus phase angle) (Fig. 10) for the substrate and TiN (2 μm) showed single and narrow peaks, indicating one time constant for the corrosion process at the substrate/electrolyte interface. However, log *f* versus phase angle showed broad peaks for the TiN (3 μm) and TiAlN (3 μm) coatings, indicating the presence of two interfaces coating/electrolyte and substrate/electrolyte due to the pitting corrosion of the coating. A similar observation has been made by William Grips *et al.*[29]

Conclusions

This study investigated the materials properties of TiAlN and corrosion resistance of TiAlN and TiN coated AISI 316L SS for clinical applications. The structural analysis using XRD reveals that the films are polycrystalline in nature, possessing a face centred cubic structure and having the lattice parameter $a=4{\cdot}2314$ nm. A dense granular structure was observed from SEM analysis. Good optical quality of these films was observed from PL studies.

Tafel plots in simulated bodily fluid showed that the corrosion rate for the specimens ranked as: AISI 316LSS (substrate)>TiN (2 μm)/substrate>TiN (3 μm)/substrate> TiAlN (2 μm)/substrate. The TiAlN coating on AISI 316L SS improved the corrosion resistance, i.e. decreasing the corrosion rate and anodic current and increasing the polarisation resistance for clinical applications. This ranking was confirmed by the EIS studies.

Table 3 Electrochemical impedance spectroscopy (EIS) data obtained for AISI 316LSS (substrate), TiN (2 μm)/substrate TiN (3 μm)/substrate, TiAlN (2 μm)/substrate

Sample	R_{ct}, Ω cm^2	C_{dl}, $\times 10^{-6}$ F cm^{-2}
AISI 316LSS (substrate)	$6{\cdot}96\times10^3$	1224
TiN (2 μm)/substrate	$1{\cdot}54\times10^4$	1164
TiN (3 μm)/substrate	$2{\cdot}51\times10^4$	725·1
TiAlN (2 μm)/substrate	$2{\cdot}62\times10^5$	82·1

Acknowledgement

One of the authors (B. Subramanian) thanks the Department of Science and Technology, New Delhi for a research grant under SERC Fast Track scheme no. SR/FTP/CS- 23/2005.

References

1. M. C. Kang, I. W. Park and K. H. Kim: *Surf. Coat. Technol.*, 2003, **163–164**, 734.
2. P. C. Jindal, A. T. Santhanam, U. Schleinlofer and A. F. Shuster: *Int. J. Refract. Met. Hard Mater.*, 1999, **17**, 163.
3. S. D. Kim, L. S. Hwang, J. K. Rhee, T. H. Cha and H. D. Kim: *Electrochem. Solid State Lett.*, 2001, **4**, G7.
4. M. Hock, E. Schaffer, W. Doll and G. Kleer: *Surf. Coat. Technol.*, 2003, **163**, 689.
5. C. T. Hanks, J. C. Wataha and S. Zhilin: *Dent. Mater.*, 1996, **12**, 186.
6. J. M. Lackner, W. Waldhauser and R. Ebner: *Surf. Coat. Technol.*, 2004, **188–189**, 519–524.
7. J. D. Bressan, R. Hesse and E. M. Silva, Jr: *Wear*, 2001, **250**, 561.
8. S. G. Harris, E. D. Doyle, A. C. Vlasveld, J. Audy and D. Quick: *Wear*, 2003, **254**, 723.
9. S. H. Ahn, J. H. Yahoo, Y. S. Choi and J. G. Han: *Surf. Coat. Technol.*, 2003, **162**, 212.
10. H.-H. Huang, C.-H. Hsu, S.-J. Pan, J.-L. He, C.-C. Chen and T.-L. Lee: *Appl. Surf. Sci.*, 2005, **244**, 252.
11. K.-L. Len, M.-Y. Hwang and D. Cheng: *Mater. Chem. Phys.*, 1996, **46**, 77–83.
12. D. Munz: *J. Vac. Sci. Technol. A*, 1986, **4A**, 2695.
13. J. Aromaa. H. Ronkainen, A. Mahiout and S. P. Hannula: *Surf. Coat. Technol.*, 1991, **49**, 353–358.

14. A. Kiruma, T. Murakami, K. Yamada and T. Suzuki: *Thin Solid Films*, 2001, **382**, 101.
15. K. Singh, A. K. Grover, K. Totlani and A. K. Suri: *Trans. IMF*, 2001, **79**, (5).
16. D. B. Lewis, S. Creasy, Z. Zhou, J. J. Forsyth, A. P. Ehiasarian, P. E. Hovsepian, Q. Luo, W. M. Rainforth and W. D. Munz: *Surf. Coat. Technol.*, 2004, **177**, 252.
17. K. N. Andersen, E. J. Bienk, K. O. Schweitz, H. Reitz and J. Chevallier: *Surf. Coat. Technol.*, 2003, **123**, 219.
18. D. B. Lewis, L. A. Donohue, M. Lembke, W. D. Munz, R. Kuzel, V. Valvoda and C. Blomfield: *Surf. Coat. Technol.*, 1999, **114**, 187.
19. M. Kong, N. Shao, Y. S. Dong, J. L. Yue and G. Y. Li: *Mater. Lett.*, 2006, **60**, 874–877.
20. Y. Li, L. Qu and F. H. Wang: *Corros. Sci.* 2003, **45**, 1367–1381.
21. H.-H. Huang, C.-H. Hsu, S.-J. Pan, J.-L. He, C.-C. Chen and T.-L. Lee: *Appl. Surf. Sci.*, 2005, **244**, 252.
22. B. Elsener, A. Rota and H. Bohni: *Mater. Sci. Forum*, 1989, **44/45**, 28.
23. G. T. Liu, J. G. Duh, K. H. Chung and J. H. Wang: *Surf. Coat. Technol.*, 2005, **200**, 2100.
24. T. S. Li, H. Li and F. Pan: *Surf. Coat. Technol.*, 2001, **137**, 225.
25. H. Mu, J. Seok and R. Y. Lin: *J. Electrochem. Soc.*, 2003, **150**, (2), c67.
26. M. H. Jacobs: *Surf. Coat. Technol.*, 1986, **29**, 221.
27. C. P. Constable, J. Yarwood and W.-D. Münz: *Surf. Coat. Technol.*, 1999, **116**, 155.
28. C. Liu, Q. Bi and A. Mathews: *Corros. Sci.*, 2001, **43**, 1953.
29. V. K. W. Grips, V. E. Selvi, H. C. Bavshilia and K. S. Rajam: *Electrochim. Acta*, 2006, **51**, 3461.